Progress in Physics Basis and its Impact on ITER

M. Shimada[1], D. Campbell[2], R. Stambaugh[3], A. Polevoi[1], V. Mukhovatov[1], N. Asakura[4], A.E. Costley[1], A.J.H. Donné[5], E.J. Doyle[6], G. Federici[7], C. Gormezano[8], Y. Gribov[1], O. Gruber[9], W. Houlberg[10], S. Ide[3], Y. Kamada[3], A.S. Kukushkin[7], A. Leonard[3], B. Lipschultz[11], S. Medvedev[12], T. Oikawa[1], M. Sugihara[1]

[1]ITER IT, Naka Joint Work Site, Naka-machi, Naka-gun, Ibaraki-ken, Japan 311-0193
[2]EFDA, [3]General Atomics, [4]JAERI, [5]FOM-Rijnhuizen, [6]PSTI UCLA, [7]ITER IT, Garching Joint Work Site, [8]ENEA Frascati, [9]IPP-Garching, [10]ORNL, [11]PSFC MIT, [12]Keldysh Institute

e-mail address: shimadm@itergps.naka.jaeri.go.jp

Abstract: This paper summarises recent progress in the physics basis and its impact on the expected performance of ITER. Significant progress has been made in many outstanding issues and in the development of hybrid and steady state operation scenarios, leading to increased confidence of achieving ITER's goals. Experiments show that tailoring the current profile can improve confinement over the standard H-mode and allow an increase in beta up to the no-wall limit at safety factors ~ 4. Extrapolation to ITER suggests that at the reduced plasma current of ~ 12MA, high Q > 10 and long pulse (>1000 s) operation is possible with benign ELMs. Analysis of disruption scenarios has been performed based on guidelines on current quench rates and halo currents, derived from the experimental database. The estimated electromagnetic forces on the in-vessel components are below the design target values, confirming the robustness of the ITER design against disruption forces.

1. Introduction

The physics basis for ITER [1] is being developed under the framework of the International Tokamak Physics Activity (ITPA). The physics understanding, projection and control methodologies developed through the ITPA after the publication of the ITER Physics Basis [2], have been summarized in a review paper [3]. A number of important results have been obtained recently in experiments, theory and modeling of tokamak plasmas. These have enabled an improved understanding of the physical processes and have given enhanced confidence in ITER achieving its goals in its integrated scenarios. They confirm that ITER will have the anticipated strong role in reactor-oriented research. This paper summarizes recent progress in the physics basis and its impact on the expected performance of ITER.

2. Inductive Operation

Experiments on many tokamaks demonstrate that H-mode confinement can be obtained at densities close to, or exceeding the Greenwald density by increasing the triangularity of the plasma cross section and by using pellet injection or impurity gas puffing [4-7]. Experimental observation of lack of beta scaling in dimensionless parameter scans [8] (which is highly favorable for high beta operation in a reactor) has been reconciled with empirical scaling laws derived from database analysis [9, 10]. New scalings have been suggested [10] that predict similar performance to existing scalings for ITER at β_N of 1.8, but much improved performance at higher β_N. Further analysis of the H-mode Threshold Database has revealed the role of aspect ratio, total B, and Z_{eff}, confirming the value of the threshold power ~40 MW obtained in the previous analysis for the reference ITER operation [11]. T_e, T_i and n_e profiles of JET were reproduced with theory-based Multi-Mode model, successfully predicting the isotope effects [12]. Attempts have been made to develop integrated models which incorporate the core, pedestal and sol/divertor regions [13, 14], and these predict Q ~ 10 in the reference inductive operation. In Ref. [13], the theory-based Multi-Mode transport model [15]

has been adopted for the core and a scaling from systematic runs of B2/Eirene [16] has been used for the sol/divertor regions. Results of dimensionless analysis, based on an appropriate JET DT discharge, support the possibility of achieving Q > 10 in ITER [17].

Inclusion of the process of elastic scattering of helium neutrals by hydrogenic ions in the divertor modelling shows that the efficiency of helium exhaust can be improved by a factor of 3-5 in ITER [18], suggesting that $\tau_{He}^*/\tau_E \sim 1.2$ may be feasible. This would lead to improvement of core performance, and, for example, to an enhanced fusion power of 500 MW with Q ~ 20 at the plasma current of 15 MA, normalized electron density $n/n_G = 0.85$ and confinement improvement factor $H_{H98(y,2)} = 1.0$ (Fig. 1).

3. Advanced Tokamak Operation

In the last few years, significant progress has been achieved in developing the Advanced Tokamak (AT) regimes with high β_N, large fraction of the bootstrap current and improved energy confinement over the H-mode scaling [19-27]. These regimes are promising for hybrid and steady state operation in ITER.

The ordinary hybrid operating mode planned for ITER is based on a combination of inductive and non-inductive current drive, leading to a long pulse operation (>1000 s) with a significant fusion power (>300 MW, Q = 5) at a medium safety factor (q_{95} = 4-5) and conservative confinement assumption ($H_{H98(y,2)} = 1$) [1]. Recently, the "improved hybrid" regimes with $H_{H98(y,2)} = 1.2 – 1.6$ have been discovered at zero or low central magnetic shear, q_0 = 1-1.5 and $q_{95} = 3.5 – 4.5$, in the absence of sawteeth [23-25]. In DIII-D these regimes were achieved at q_{95} as low as 3.2 with small sawteeth [25]. The quasi-stationary improved hybrid regimes with ~50% non-inductive current fraction at $\beta_N \sim 3$ that is close to the no-wall beta limit ($\beta_N \sim 4l_i$) have been obtained in ASDEX Upgrade, DIII-D, JET and JT-60U [20-26]. Such discharges show usually peaked density profiles especially near the ITER ν^* values, although the energy confinement does not correlate strongly with the density peaking [26]. The confinement increases with T_{io}/T_{eo} or toward lower density, yet showing $H_{89} \sim 1.8$ at $T_{io}/T_{eo} \sim 1$ [26]. New JET experiments with a large component of RF heating have shown that injected momentum is not essential and that these regimes are compatible with very low edge activity [20]. The improved hybrid regimes have been obtained in JET at low ρ^* (~3 x 10^{-3}). However, the β_N values achieved so far are moderate (1.1-1.6), probably due to low heating power. In ASDEX Upgrade, $H_{H98(y,2)} = 1.2$ is achieved at $n/n_G = 0.85$ [27]. If ITER achieved similar normalised parameters, fusion powers of ~ 350 MW, Q > 10 would be achieved at $\beta_N \leq 2.2$ (Fig. 2). The required β_N is well below the no-wall ideal MHD limit for resistive wall mode. A burn time longer than 1000 s with Q ~ 20 would be expected (Fig. 2). This operation scenario is a potential candidate for an operation mode with high Q, long pulse and benign ELMs.

For the steady state (SS) operation, the total plasma current at the current flat-top phase should be generated non-inductively by the bootstrap effect, neutral beam injection and RF waves. SS scenarios rely upon discharges with a relatively low plasma current, high safety factor $q_{95} \geq 4$, improved confinement ($H_{H98(y,2)} \geq 1.3$) and high beta ($\beta_N \geq 2.5$). The improved confinement is expected to be achieved, e.g. in reversed-shear operation. Stationary operation has been obtained experimentally at $q_{95} \geq 5$, with the maximum performance just in line with ITER requirements for steady state operation at Q ~ 5 [26]. Database analysis shows that achieved beta decreases at pressure profile peaking [26], indicating the need of pressure profile control. In JT-60U, a high fusion triple product, $n\tau_E T$, has been sustained in steady-state with $\beta_N = 2.4$ and $q_{95} = 4.1$ at a collisionality close to that in ITER, and a high beta

plasma (β_N = 2.7) has been sustained for 7.4 s ($\approx 60\tau_E$) in discharges with a weak positive shear and q_0 = 1-1.5 [22]. A clear ITB has not been identified and impurity accumulation has not been observed in this mode. Example scenarios for the SS operation in ITER are as follows:

1) 9-10 MA, NB+LH, RS, $H_H \sim 1.3$-1.5, $\beta_N \sim 2.5$, $Q \sim 5$ [28]
2) 12 MA, NB+LH, RS, $H_H \sim 1.5$, $\beta_N \sim 3.6$, $Q \sim 8$ (P_{fusion} = 0.7 GW) [28]
3) 9 MA, NB+EC, WS, $H_H \sim 1.5$-1.7, $\beta_N \sim 2.7$, $Q \sim 5$ (Fig. 3) [29].

Operation in these regimes requires strong plasma shaping and simultaneous control of the current and pressure profiles and active control of RWMs and possibly NTMs. Code benchmarking and validation of NBCD, ECCD and LHCD models, which are very important for projection for these regimes, have been undertaken and good agreement has been obtained [30]. Simulations of ITER steady-state scenario with the GLF23 transport model [30, 31], suggest that SS operation with $Q \sim 5$ is feasible with 33 MW NBCD, 20 MW FWCD and 20 MW ECCD at a rather high densities of $\sim 1 \times 10^{20}$ m^{-3} and high pedestal temperature of 7 keV [30]. The GLF transport model has been validated against recent DIII-D experiments that aim at fully non-inductive operation at high beta. The T_e, T_i and toroidal momentum profiles, calculated with density profiles fixed to experimental measurements, show good agreement with experimental profiles [30, 31]. In [32], GLF transport model has been shown to predict temperature profiles of DIII-D, JET and ASDEX Upgrade rather well, taking the density and toroidal rotation profiles from experimental data. The requirements on fuelling in these scenarios have been investigated with the ASTRA code [29]. It is shown that the DT pellet throughput of ~50 Pam^3/s will be required in SS scenarios, which is inside the ITER design value (100 Pam^3/s).

Many areas require further work, in particular, the extrapolation of improved hybrid regimes to lower ρ^*, the size scaling of ITB formation and sustaining ITBs at high plasma density, $T_i \sim T_e$ and slow toroidal rotation with prevention of impurity accumulation.

4. Neoclassical Tearing Mode

Neoclassical Tearing Mode (NTM) suppression by localized EC current drive for both 3/2 and 2/1 modes has been successfully demonstrated in experiments. A real-time NTM stabilization system has been developed where detection of the centre of the magnetic island and optimization of the injection angle of the electron cyclotron wave are performed in real time [22]. Projection to ITER suggests that an EC beam with power of ~30 MW would be sufficient to stabilize both the 3/2 and 2/1 NTMs [33]. Injection when the island size is small reduced the required ECCD power [34]. An EC beam narrower by a factor of two is expected to reduce the power required for NTM suppression by a factor of ~ 4.

5. Resistive Wall Mode

In DIII-D, it was shown that resistive wall modes (RWM) can be stabilized at high beta above the no wall limit by a resistive wall, with sufficient plasma rotation and without feedback control [35]. The rotation speed required for stabilization derived experimentally and theoretically is ~ 2 % of the Alfvénic speed. The resonant response to error fields by a marginally stable resistive wall mode can lead to strong damping of the rotation. The error-field correction capability in ITER could enable stabilization of the RWM by rotation especially when the rotation is large. However, the rotation speed in the steady state plasmas

in ITER estimated with the ASTRA code is somewhat lower than this value. Therefore feedback stabilization of the RWM by saddle coil is implemented.

The suppression of RWMs has been investigated for ITER steady state scenarios [36]. A multi-input, multi-output linear quadratic Gaussian (LQG) controller has been produced on the basis of a semi-analytical model of RWM developed by Y.Q. Liu and A. Bondeson with the MARS-F code [37] treating the configuration of the plasma, saddle coils and vacuum vessel. An analysis shows that this controller, without using the second time derivative of the field, is able to suppress highly unstable modes with $C_\beta \sim 0.8$ ($C_\beta = (\beta_N - \beta_N(\text{no wall}))/(\beta_N(\text{ideal wall}) - \beta_N(\text{no wall}))$) with coil voltages of about 300 V/turn, which is implemented in ITER.

6. Plasma-Wall Interaction

Experimental characterization of type-I ELMs has confirmed [38] that the transport nature is conductive (convective) in low (high) collisionalities [39]. Measurements in JET indicate that a significant portion of the energy flux to the divertor takes place over a relatively long time scale so that the fraction of ELM energy flux that causes the sudden temperature rise is in the region 20-40%, with lower values for more convective ELMs. If convective ELMs can be achieved in ITER, the expected energy flux density corresponds to ~ 20 MJ $m^{-2} s^{-1/2}$, which is a factor of two below the CFC ablation threshold (45 MJ $m^{-2} s^{-1/2}$). On the other hand, in the case of conductive ELMs, the expected heat load corresponds to ~ 70 MJ $m^{-2} s^{-1/2}$, which results in short lifetime of the target. Measurements in ASDEX-Upgrade indicate ~ 50 % of the ELM heat load is deposited on a narrow area on the divertor targets [40]. If this result can be applicable to ITER, the divertor heat load corresponds to ~ 35 MJ $m^{-2} s^{-1/2}$, below the ablation threshold. Power fluxes on the ITER divertor targets associated with Type I ELMs could be close to or above marginal for an acceptable divertor lifetime [41], which has motivated development of back-up scenarios. Potential scenarios include those with more frequent, smaller ELMs triggered by frequent pellet injection [42], and regimes with benign or no ELMs (including QH-mode, EDA and improved hybrid mode).

Tritium retention control remains a key issue, requiring more efforts on the investigation of retention mechanism and development of efficient removal techniques [43]. In ITER, a design target of 350 g is set on the maximum tritium retention inside the vacuum vessel. Transport calculations suggest that an inductive operation requires 50 Pa m^3/s of T fuelling during a DT burn, which corresponds to 54 g of tritium for a discharge with 400 s burn. Experiments in JET and TFTR suggest that ~ 30 % of tritium injected is retained in the vessel with C walls and divertor targets. If we assume that 30 % of injected T is retained in the vessel, 9000 s burn at a fusion power of 400 MW can run before the T retention reaches 350 g. A model calculation suggests that the tritium retention increases at a rate of 2-5 g/discharge in ITER [44], which will enable operation of 28000-70000 s burn at a fusion power of 400 MW is available before the T retention reaches 350 g. Further, PISCES experiments suggest that the build-up of tritium retention could be significantly reduced (~ x 1/5) by the coverage of carbon surface by beryllium [45]. A number of T removal techniques have been tested. For example, an ICRF discharge is expected to remove 350 g of tritium in ~ 10 days. This requirement can be reduced significantly if ICRF cleaning can be implemented after every DT shot. However, a challenge is to remove tritium from shadow areas, not accessible by a plasma. These considerations suggest that tritium retention could be controlled during the physics operation phase with a low fluence. But a fundamental improvement is required for high fluence operation.

Elimination of graphite from the vessel would be attractive from a viewpoint of tritium retention control. However, experiments with tungsten in ASDEX-Upgrade show that tungsten can accumulate in the center in discharges with ITB, in the absence of sawtooth/fishbones and frequent ELMs (near the L-H threshold). High central heating could suppress the accumulation [46], but the heating power required to suppress the density peaking and impurity accumulation needs to be assessed. The combination of CFC targets and beryllium walls is expected to facilitate operation with a wide range of parameters, which is essential for the initial operation.

7. Disruption

Analysis of disruption scenarios has been performed based on guidelines on current quench rates and halo currents, derived from an experimental database. The estimated electro-magnetic forces on the in-vessel components are below the design values [47], confirming the robustness of the ITER design against disruption forces for the operation with plasma currents up to 15 MA. The experimental database shows that a significant fraction of stored energy (< 50% in JET [48], 30-100 % in ASDEX Upgrade[49] and 50-100 % in DIII-D [2]) is deposited on the divertor plates at the thermal quench. The deposition area is ~ 3 times the area of the wetted surface during the normal phase, sometimes larger. The estimated thermal loads in ITER indicate that the tungsten would melt, if used for the divertor targets. The melting would create rough surfaces of tungsten, which would melt during normal operation, restricting the parameter space to a high-density regime. Therefore the initial divertor target material will be CFC, which is much more robust against disruption loads. This will enable operation with a wide range of parameter space, which is required in the initial operation. Disruption prediction methods with neural network [50] and disruption mitigation techniques with massive gas injection have been proposed [51]. High-Z metal target plates (e.g. tungsten) could be installed after methodologies have been established for disruption prediction and mitigation and suppression of impurity accumulation. This would be advantageous from the viewpoint of tritium retention control.

8. Energetic Particles

One of the major scientific goals for ITER is to demonstrate and investigate burning plasmas, in which a significant power is produced by the DT fusion reactions. Such plasmas are characterized by a large isotropic population of fusion alphas, providing the dominant heating of the plasma. The energetic ions can be susceptible to ripple-induced loss. However, from Monte-Carlo calculations it is known that the ripple-induced loss can be reduced to a negligible level by introducing ferritic inserts into the vacuum vessel [52], which are implemented in ITER. The energetic alpha particles can induce collective modes, such as fishbones, Toroidal Alfvénic Eigenmodes (TAEs) and Energetic Particle Modes (EPMs), which could redistribute the alphas across the plasma or result in loss of alphas.

A non-linear modeling of fishbones [53] produces a downshifting frequency sweep, which is similar to experimental observation. The MHD non-linearities can explain the explosive initial growth of fishbone pulse and frequency chirping [54]. For the fishbone oscillations that are excited well above the stability threshold, the growth rates decrease non-linearly. As the usual fishbone mode occurs near the q=1 surface deep within the plasma, the loss of alpha particles from a fishbone is not expected to be severe since alpha particle orbits (≤15 % of the minor radius in ITER) are not large enough to reach the plasma edge.

Recurrent bursts of TAE and energetic ion loss have been studied theoretically and numerically [55]. The results of the simulation reproduced the time intervals between the bursts and a modulation depth in the stored beam energy. However, there remain discrepancies in saturation amplitude between the experimental observations and the simulation results.

As shown in Ref. [56], the non-linear Alfvén mode dynamics gradually change from the weak non-linear AE behaviour, due to wave-particle trapping, to the strong non-linear regime and typical of EPM. Dedicated studies of energetic particle transport in reversed shear scenarios have demonstrated that lower q_{min} values, more centrally located in the plasma column, and higher q_{min}'' (second order radial derivative of q at the minimum q) are preferable and yield smaller EPM induced energetic particle losses [57].

The theoretical description of non-linear EPM dynamics fits well with the experimental observation of Abrupt Large amplitude Events (ALE) [58] on JT-60U. These are Alfvénic oscillations with poloidal amplitude $\delta B_\theta / B_\theta \sim 10^{-3}$, characteristic time scale of $200 \div 400 \mu s$ and strong frequency chirping [59]. These modes are responsible for a $\leq 15\%$ drop in the neutron rate with a corresponding increase in the energetic particle loss signal [59]. Experimental measurements also indicate macroscopic fast ion radial redistribution in the plasma core [57] with very similar features to those evidenced in numerical simulations.

The presence of so-called grand Alfvén cascades allows an observer to infer that the discharge is likely to be shear reversed and how fast the minimum q-value is changing. The emergence of grand cascades (where all the n-numbers appear almost simultaneously) indicates that the minimum q-value is at a rational surface. This knowledge has enabled JET experimentalists to trigger transport barriers in an efficient manner [60].

According to the analysis based on the non-local gyrokinetic code calibrated against the n = 1 mode observed in JET, the alpha-driven, radially extended TAEs with n = 1-12 should be stable in the ITER nominal inductive scenario [61]. NOVAK analysis of Alfvén Eigenmode shows that n = 10-12 are unstable and injection of 1 MeV neutral beam would make n = 7-17 unstable in the ITER nominal inductive scenario [62]. However, the neutral beam is assumed to go through the plasma center. The calculation should be undertaken again with the correct beam configuration, where the neutral beam is vertically shifted. In configurations with reversed shear, drift-kinetic Alfven Eigenmodes and Energetic Particles Modes could be made unstable [61], which could set an upper limit to the minimum q-value in ITER.

Acknowledgement

Fruitful discussion with Dr. Shimomura of ITER IT, Prof. H Bolt of IPP Garching and Dr. F. Zonca of ENEA Frascati is gratefully acknowledged.

References

[1] ITER Technical Basis, ITER EDA Documentation Series No. 24, IAEA, Vienna, 2002.
[2] ITER PHYSICS BASIS EDITORS et al 1999 Nucl. Fusion **39** 2175.
[3] International Tokamak Physics Activity Topical Groups, Nucl. Fusion to be published
[4] MAHDAVI A M et al 2002 Nucl. Fusion **42** 52
[5] ONGENA J et al 2004 Nucl. Fusion **44**, 124
[6] FUJITA T et al 2003 Nucl. Fusion **43** 1527
[7] LANG P T et al 2002 Plasma Phys. Control. Fusion **44** 1919
[8] PETTY C C et al 2004 Phys. Plasmas 2514
[9] THOMSEN K et al 2004 Proc. 31st EPS Conf. on Plasma Phys. ECA Vol.**28G**, P-5.145
[10] CORDEY JG et al this Conference IT/P3-32
[11] TAKIZUKA T et al 2004 Plasma Phys. Control. Fusion **46** A227
[12] BATEMAN G et al 1999 Phys. Plasmas **6** 4607
[13] PACHER G W et al 2004 Plasma Phys. Control. Fusion **46** A257
[14] BATEMAN G et al 2003 Plasma Phys. Control. Fusion **45** 1939
[15] BATEMAN G et al 1998 Phys. Plasmas **5** 1793
[16] PACHER H D et al 2003 J. Nucl. Mat. **313-316C** 657
[17] MUKHOVATOV V et al 2003 Plasma Phys. Control. Fusion **45** A235
[18] KUKUSHKIN A et al 2002 Plasma Phys. Control. Fusion **44** 931
[19] GREENFIELD C M et al GA-A24762, to be published in Plasma Phys. Control. Fusion
[20] GORMEZANO C et al to be published in Plasma Phys. and Contr. Fusion
[21] CONNOR J W et al 2004 Nucl. Fusion **44** R1
[22] ISAYAMA A et al 2003 Nucl. Fusion **43** 1272
[23] SIPS A C C et al 2002 Plasma Phys. Control. Fusion **44** B69
[24] WADE M R et al 2002 29th EPS Conf. on Plasma Phys. and Contr. Fusion ECA Vol. **26B**, O-2.08
[25] LUCE T C et al 2004 Phys. Plasma **11** 2627
[26] SIPS A C C et al this Conference IT/P3-36
[27] SIPS A C C et al 2003 30th EPS Conf. on Contr. Fusion and Plasma Phys. ECA Vol. **27A**, O-1.3A
[28] POLEVOI A et al 2002 Proc. 19th IAEA Fusion Energy Conf. CT/P-08
[29] POLEVOI A et al this Conference IT/P3-28
[30] HOULBERG W et al this Conference IT/P3-33
[31] MURAKAMI M et al this Conference EX/1-2
[32] KINSEY J et al this Conference IT/P3-37
[33] PUSTOVITOV V D et al 2000 18th IAEA Fusion Energy Conf. ITERP/07
[34] NAGASAKI K et al 2003 Nucl. Fusion **43** L7
[35] STRAIT EJ 2003 Nucl. Fusion **43** 430
[36] GRIBOV Y et al this Conference IT/P3-22
[37] LIU Y and Bondeson A 2004 Nucl. Fusion **44** 232
[38] LOARTE A et al 2004 Phys. Plasma **11** 2668
[39] LEONARD A W et al 1999 J Nucl. Mat. **266-269** 109
[40] HERRMANN 2004 Plasma Phys. Control. Fusion **46** 971
[41] FEDERICI G et al 2003 Plasma Phys. Control. Fusion **45** 1523
[42] LANG P T et al 2003 Nucl. Fusion **43** 1110
[43] PHILIPPS V et al 2003 Plasma Phys. Control. Fusion **45** A17
[44] FEDERICI G et al 2002 Proc. 19th Symposium on Fusion Eng.
[45] SCHMID K et al 2004 Nucl. Fusion **44** 815
[46] NEU R et al 2003 Proc. 30th EPS ECA **27A** P-1.123

[47] SUGIHARA M et al this Conference IT/P3-29
[48] ANDREW P et al 2003 Proc. 30th EPS Conf. on Contr. Fusion and Plasma Phys., ECA Vol. **27A**, P-1.108
[49] PAUTASSO G et al 2004 Proc. 31st EPS Conf. On Plasma Phys. ECA Vol. **28G**, P-4-132
[50] YOSHINO R 2003 Nucl. Fusion **43** 1771
[51] WHYTE D G et al 2003 J. Nucl. Mat. **313-316** 1239
[52] TOBITA K et al 2003 Plasma Phys. Control. Fusion **45** 133
[53] CANDY J et al 1999 Phys. Plasma **6** 1822
[54] ÖDBLOM A et al 2002 Phys. Plasma **9** 155
[55] TODO Y., BERK H.L. and BREIZMAN B.N. 2003 Phys. Plasmas **10** 2888
[56] ZONCA F et al 2002 Phys. Plasmas **9** 4936
[57] BRIGUGLIO S et al 2002 Phys. Lett. A **302** 308
[58] SHINOHARA K et al 2002 Nucl. Fusion **42** 942
[59] SHINOHARA K et al 2001 Nucl. Fusion **41** 603
[60] JOFFRIN E et al 2003 Nucl. Fusion **43**,1167
[61] JAUN A et al 2002 IAEA Fusion Energy Conference CT/P-06
[62] GORELENKOV N N et al 2003 Nucl. Fusion **43** 594

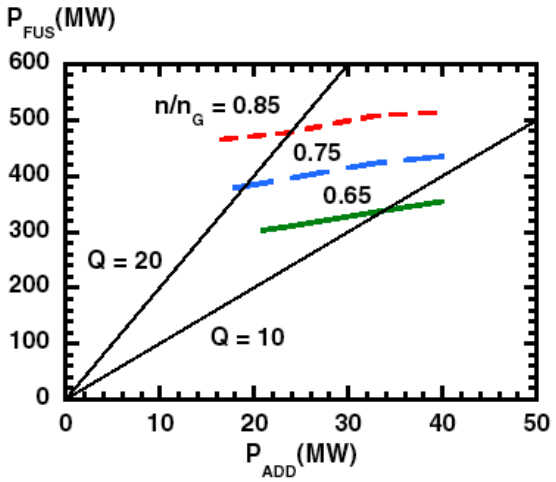

Fig. 1 Fusion power vs. additional heating power with a plasma current of 15 MA

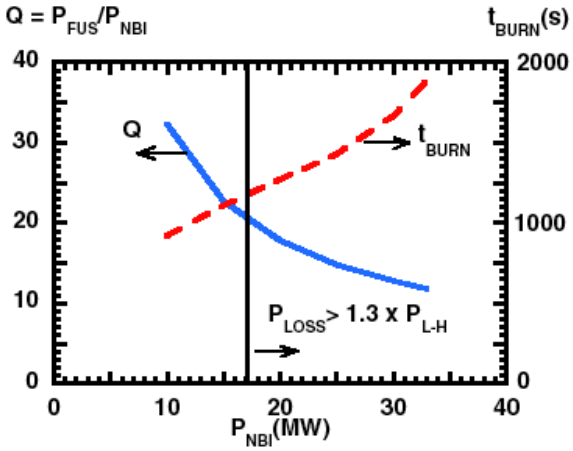

Fig. 2 Fusion gain and burn time vs. NBI power with a plasma current of 12 MA at HH = 1.2 and density of 85% of Greenwald density

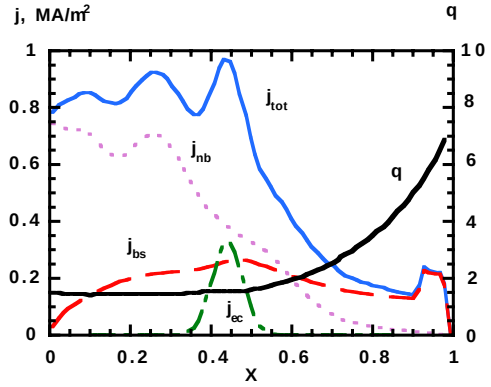

Fig.3 Current density and safety factor profiles for the SS equilibrium with β_N^{SS} *=2.67,* $q_0 / q_{min} / q_{95}$ *=1.6/1.45/5.25,* $p_0/\langle p \rangle$ *=3.5,* l_i *=0.8 with the initial current drive systems, i.e. 33 MW NB and 20 MW EC.*